scientific reports

Check for updates

OPEN

System biology-based assessment of the molecular mechanism of IMPHY000797 in Parkinson's disease: a network pharmacology and in-silico evaluation

Gomathy Subramanian[1], Hannah Lalengzuali Fanai[1], Jagdish Chand[1]✉, Sheikh F. Ahmad[2], Sabry M. Attia[2] & Talha Bin Emran[3,4,5]✉

IMPHY000797 derivatives have been well known for their efficacy in various diseases. Moreover, IMPHY000797 derivatives have been found to modulate such genes involved in multiple neurological disorders. Hence, this study seeks to identify such genes and the probable molecular mechanism that could be involved in the pathogenesis of Parkinson's disease. The study utilized various biological tools such as DisGeNET, STRING, Swiss target predictor, Cytoscape, AutoDock 4.2, Schrodinger suite, ClueGo, and GUSAR. All the reported genes were obtained using DisGeNET, and further, the common genes were incorporated into the STRING to get the KEGG pathway, and all the data was converted to a protein/pathway network via Cytoscape. The clustering of the genes was performed for the gene-enriched data using two-sided hypergeometrics (p-value). The binding affinity of the IMPHY000797 was verified with the highest regulated 25 proteins *via* utilizing the "Monte Carlo iterated search technique" and the "*Emodel and Glide score*" function. Three thousand five hundred eighty-three genes were identified for Parkinson's disease and 31 genes for IMPHY000797 compound, among which 25 common genes were identified. Further, the "FOXO-signaling pathway" was identified to be a modulated pathway. Among the 25 proteins, the highest modulated genes and highest binding affinity were exhibited by SIRT3, FOXO1, and PPARGC1A with the compound IMPHY000797. Further, rat toxicity analysis provided the efficacy and safety of the compound. The study was required to identify the probable molecular mechanism, which needs more confirmation from other studies, which is still a significant hit-back.

Keywords Network pharmacology, Parkinson's disease, Neuroprotection, *In-silico* studies, IMPHY000797

Parkinson's Disease (PD) is a progressive degeneration of dopaminergic neurons in the brain, manifested by motor and non-motor symptoms[1]. Bradykinesia, rigidity, postural instability, and autonomic dysfunction are some of the symptoms that are produced in PD patients[2]. Numerous natural molecules have presented their potency in countering reactive oxygen species levels (ROS), and oxidative stress, resulting in neuroprotection[3]. The unexplored IMPHY000797 (pyrimidine) derivatives have become highlighted due to their notable actions on neurodegenerative diseases such as monoamine oxidase inhibitors, Alzheimer's disease, and PD[4–7]. Due to its unexplored action on neurodegenerative diseases, the proper molecular mechanism action remains unexplored for neurodegenerative diseases, as shown in Fig. 1[8].

One of the main culprits in the progression of PD remains to be ROS and oxidative stress generating *via* the mitochondrial route; both in-vitro and in-vivo model studies have exhibited the effective role of mitochondria as how the upregulation of various genes can enhance the mitochondrial activity and result in neuroprotection's[9,10].

[1]Department of Pharmaceutical Chemistry, JSS College of Pharmacy, JSS Academy of Higher Education & Research, Ooty 643001, Tamil Nadu, India. [2]Department of Pharmacology and Toxicology, College of Pharmacy, King Saud University, Riyadh 11451, Saudi Arabia. [3]Department of Pathology and Laboratory Medicine, Warren Alpert Medical School, Brown University, Providence, RI 02912, USA. [4]Legorreta Cancer Center, Brown University, Providence, RI 02912, USA. [5]Department of Pharmacy, Faculty of Allied Health Sciences, Daffodil International University, Dhaka 1207, Bangladesh. ✉email: sachinchand190@gmail.com; talha_bin_emran@brown.edu

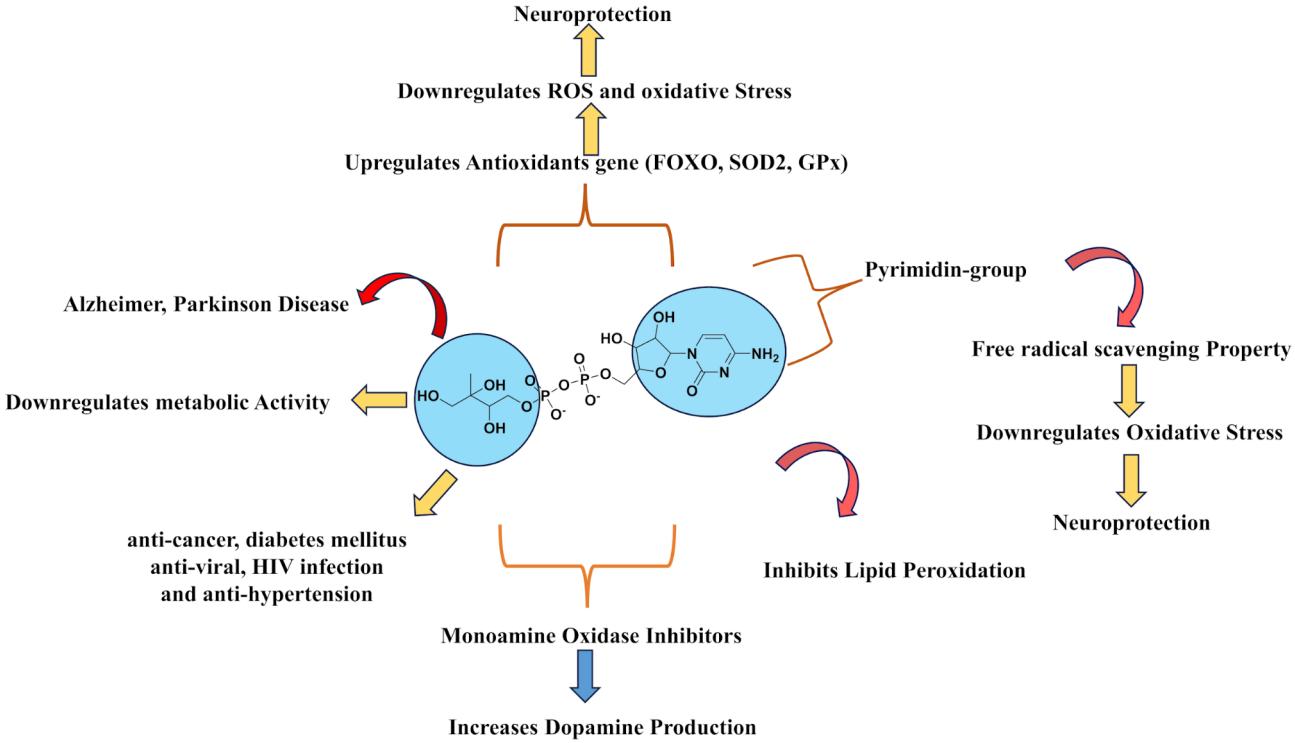

Fig. 1. IMPHY000797 and its multiple involvements in the pathogenesis of diseases.

Due to the advancement of biological tools, wet lab work has improved in past decades, improving the effectiveness between target and compound[11]. As reported, IMPHY000797 moieties have been studied for neuroprotection; in this contextual manner, we have utilized several biological tools to identify the probable molecular mechanism of IMPHY000797 concerning ROS levels and oxidative stress *via* studying various genes.

Materials and methods

Physicochemical properties of the IMPHY000797 compound

The compound was retrieved using PubChem, Indian Medicinal Plants (IMPPAT), whereas the MolSoft LLC database (https://www.molsoft.com/) was used to identify the drug-likeness score (DLS) of the drug. The physicochemical properties include a DLS of 0.81, a molecular weight of 521.08 with a hydrogen bond acceptor, and a donor of 15 and 9. The targets involved in the modulation of PD were retrieved using the DisGeNET database (https://www.disgenet.org/) CUI: C3825201, CUI: C0030567, CUI: C0751651, CUI: C0949855 with an overall gene count of 3583[12]. The modulating targets for IMPHY000797 were predicted using SMILES in Swiss target prediction (http://www.swisstargetprediction.ch/), which predicted the common gene count 31.

Gene Ontology (GO) enrichment

The biological process (BP), molecular function (MF), and cellular component (CC) were retrieved using the STRING database, where the highest modulated gene was identified. Moreover, a two-tailed Pearson correlation coefficient analysis was performed for the GO terms using GraphPad Prism 8.

Network construction

The targets obtained from the DisGeNET database, CUI: C3825201, CUI: C0030567, CUI: C0751651, and CUI: C0949855, were cross-matched with the genes obtained from Swiss target prediction for IMPHY000797. The common targets were further adapted into protein-protein interaction using STRING databases for "homo-sapiens"[13].

Clustering and its analysis

The ClueGO, an additional tool, was utilized to obtain the single clustering analysis from a set of multiple genes in Cytoscape 3.10.0[14]. The critical points analyzed for clustering were BP, MF, CC, and KEGG pathways[15]. In contrast, the Two-sided hypergeometric test (enrichment/depletion) statistical analysis was performed with a P-value range of 0.05. The network specificity was medium with a GO tree interval of 3 to 8. The final Kappa score was obtained as 4, and the analysis was performed under the Bonferroni step-down method.

Preparation of the IMPHY000797 compound

IMPHY000797 (an IMPHY000797-based compound): The ligand was prepared using ChemDraw 19.0, saved in .mol format, and minimized using ChemDraw 3D using the MM2 force field. The file was converted to pdb. and pdbqt. Format (charged ligand)[16]. The "LigPrep" module (glide/Schrodinger suite) was used (glide/Schrodinger suite) to obtain the probable confirmations of the ligand, where the pH was kept in the range of 7.0 ± 0.2 using OPLS4 forcefield[17].

Preparation of protein for AutoDock 4.2

All the proteins were extracted using Protein Data Bank, RCSB (https://www.rcsb.org/), and the extracted proteins were prepared using BIOVIA Discovery Studio-2017, where the water molecules and unwanted heteroatoms were removed, and the missing amino acids were substituted to the protein. The prepared protein was substituted with polar hydrogens, followed by Gasteiger and Kollmann charge, and converted into pdbqt. Format. Further "grid box" was established by using the "center of the macromolecule" in "AutoDock 4.2"[18].

Preparation of protein for Schrodinger suite and molecular Docking studies

The "protein-preparation wizard tool" of the Schrodinger Suite 2022-24 was utilized to prepare protein. The unwanted water molecules were removed with OPLS4 and RMSD of 0.30 Å. The "PROPKA" module was used in the optimization of hydrogen bonds; further, the "grid" was formed using the "receptor-grid generation" tool. In the present study, the IMPHY000797 compound was docked with a hydrolase enzyme (Human SIRT3 bound to Ac-ACS peptide and Carba-NAD), PDB ID:4FVT, with the 2.47 Å. The docking was executed using the "ligand-docking" tool with XP (extra precision) to obtain the binding affinity of the compound with the selected PDB ID[19]. The docking was performed using two computational algorithms, AutoDock 4.2 and Schrodinger suite (glide).

Trajectory studies

Selection of proteins for the simulation stability studies

Among the large set of proteins, the highest number of edge counts were obtained by SIRT3/FOXO1 and PPARGC1A. The "system builder" was utilized in the solvation of the protein-ligand complex, where the "TIP4P" was used as a solvent, and the buffer was added within a distance of 10/10/10 Å. The model was minimized using the neutral Na + ions *via* the OPLS4 forcefield. The protein-ligand complex was further minimized at 100 picoseconds, and the residues of the protein-TIP4P compound were simulated at 100 nanoseconds under a pressure of 1.01 at 311 K temperature[20].

Rat acute toxicity

The "GUSAR" (General Unrestricted Structure-Activity Relationships) (https://www.way2drug.com/gusar/acutoxpredict/) module was used to predict acute toxicity. The GUSAR module predicts acute toxicity by running over 10 K chemical entities, whereas the QSAR approach was used to estimate acute toxicity[21].

Results and discussions

IMPHY000797 and its physicochemical properties

IMPHY000797 was determined to have a molecular weight of 521.08 Daltons and a log-p value of -3.2, with two hydrophobic rings; the NHBA and NHBD were found to be 15 and 8, respectively. The DLS score was found to be 0.81. Thirty-one genes, HDAC1, SOD2, FOXO1, PPARGC1A, UBB, AMPK, IDH2, NTRK2, CREBBP, SIRT3, CDC34, PRKAA2, ATP5F1B, MAP4K4, PRKAA1, CDK1, PDE2A, ALOX5, IGF1R, HSD11B1, PTGS1, RELA, ESRRB, EPHX2, HMGCR, MAP2K1, ADORA1, NTRK1, NTRK3, PRKDC, HIF1A, were found to be modulated by the compound IMPHY000797, and 3583 of genes were found to be involved in the modulation of PD which was obtained using DisGeNET database. The common genes were identified from both sets (compound genes and DisGeNET genes) which predicted 25 common genes (HDAC1, SOD2, FOXO1, PPARGC1A, UBB, NTRK2, CREBBP, SIRT3, CDC34, PRKAA2, ATP5F1B, MAP4K4, PRKAA1, CDK1, PDE2A, ALOX5, IGF1R, RELA, EPHX2, MAP2K1, ADORA1, NTRK1, NTRK3, PRKDC, HIF1A) as shown in Fig. 2.

Gene enrichment analysis for IMPHY000797 and network construction

The genes modulated in the PD were obtained using the DisGeNET database with the access codes "CUI: C3825201, CUI: C0030567, CUI: C0751651, and CUI: C0949855". Whereas targets modulated by the IMPHY000797 compound (IMPHY000797) were obtained using Swiss target prediction (http://www.swisstargetprediction.ch/) and Binding database (https://www.bindingdb.org/rwd/bind/index.jsp), which were having a probable score of 0.5-1. Overall, of 3583 genes were obtained using DisGeNET database, whereas the compound IMPHY000797 was found to modulate 31 genes (HDAC1, SOD2, FOXO1, PPARGC1A, UBB, AMPK, IDH2, NTRK2, CREBBP, SIRT3, CDC34, PRKAA2, ATP5F1B, MAP4K4, PRKAA1, CDK1, PDE2A, ALOX5, IGF1R, HSD11B1, PTGS1, RELA, ESRRB, EPHX2, HMGCR, MAP2K1, ADORA1, NTRK1, NTRK3, PRKDC, HIF1A). Furthermore, the commonly predicted 25 genes were queried in the STRING database (https://string-db.org/) to analyze the probable protein-protein interactions. The threshold used to choose high-confidence protein-protein interactions from the "STRING" database was set to "0.700," which can be found in the "settings" section of the STRING database. Protein-protein interactions can be classified as highly confident if the high confidence factor exceeds 0.700. There were 25 nodes and 63 edges. The average node degree was determined to be 2.61, with a clustering value of 0.62. The protein-protein enrichment p-value was 4.33e-1, indicating that the proteins had many interactions. This enrichment suggested that the targets were physiologically related to each other. Eighty-one enriched KEGG pathways were obtained (Supplementary File

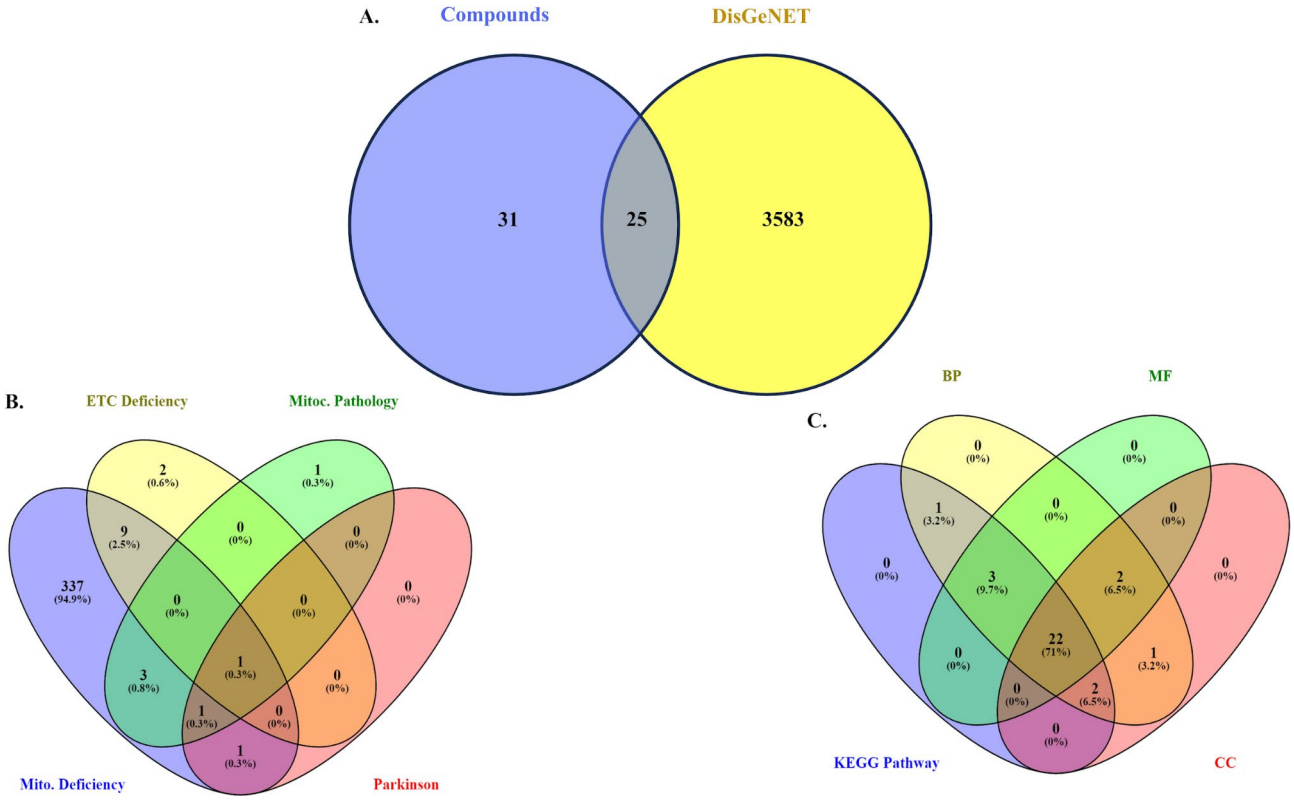

Fig. 2. Venn illustration representation. (**A**) Targets involved in the modulation of PD (CUI: C0949855) and targets modulated by the IMPHY000797 compound. (**B**) Multiple sets of 3583 genes were collected from the different keywords involved in the pathogenesis of PD (CUI: C3825201, CUI: C0030567, CUI: C0751651, and CUI: C0949855). (**C**) The GO terms Biological Process (BP), Molecular function (MF), and Cellular component (CC) via KEGG-mediated pathways.

1)[22,23]. Figure 3 illustrates how the network between the gene/pathways and compound targets was built using "Cytoscape 3.10.0". SIRT3/FOXO1 and PPARGC1A displayed the highest number of "edge counts" among all the genes with a neighborhood connectivity of 6.4, the "FOXO signaling pathway" was found to have an edge count of 7, followed by an in-degree of 3, and an outdegree of 6.

Gene Ontology (GO) and Pearson correlation analysis

The GO term analysis predicted 56 KEGG pathways, whereas the "Longevity regulating pathway" was found to have a false discovery rate (FDR) of 3.57E-08. The KEGG pathway also predicted the "FOXO signaling pathway" (hsa04068) with an FDR of 1.41E-07, indicating probable significance, which could have resulted in more false results. A total of 175 BP was determined, among which "Cellular response to oxidative stress" (GO:0034599) and "Response to oxidative stress" (GO:0006979) were found to have the lowest FDR of 1.44E-06 and 8.98E-09 and were found to modulate eight proteins (PPARGC1A, SIRT3, PRKAA2, FOXO1, CDK1, RELA, HIF1A, SOD2). The 29 MF were predicted, among which "Small molecule binding" (GO:0036094) was predicted with an FDR of 5.11E-07, whereas it was found to modulate 19 proteins (CDC34, ATP5F1B, NTRK2, HMGCR, MAP2K1, PRKDC, IDH2, PDE2A, MAP4K4, FOXO1, NTRK3, HSD11B1, ADORA1, PRKAA2, SIRT3, CDK1, NTRK1, SOD2, IGF1R). Overall, of 7 CF were predicted, among which "Cytoplasm" (GO:0005737) was found to modulate 31 genes (CDC34, ATP5F1B, CREBBP, PPARGC1A, NTRK2, HMGCR, MAP2K1, PRKDC, IDH2, PDE2A, MAP4K4, PRKAA1, NTRK3, PTGS1, HSD11B1, ADORA1, PRKAA2, HDAC1, ALOX5, FOXO1, ESRRB, SIRT3, CDK1, RELA, EPHX2, CA1, NTRK1, HIF1A, SOD2, UBB, IGF1R). All the enrichment analyses predicted various common genes, among which SIRT3, FOXO1, and PPARGC1A were identified as the most common genes involved in the modulation of oxidative stress. The diagram has been presented as a violin plot, which indicates the top-most modulated genes throughout the enrichment analysis, as shown in Fig. 4.

The Pearson correlation matrix statistical analysis was performed for the GO terms BP, MF, and CC. The predicted Pearson correlation for BP at 95% between the "observed gene count vs strength" was found to be -0.834 and −0.717 with a two-tailed p-value < 0.0001 (****). In contrast, the correlation between "observed gene count vs false discovery rate" was found to be -0.604 and −0.380 with a two-tailed p-value < 0.0001 (****). The predicted Pearson correlation for MF at 95% between the observed gene count vs. strength was found to be -0.919 and −0.663 with a two-tailed p-value < 0.0001 (****). In contrast, the correlation between "observed gene count vs false discovery rate" was found to be -0.639 and 0.030 with a two-tailed p-value of 0.071, indicating no significance; it means that there was a lack of statistical significance between the "observed gene count vs

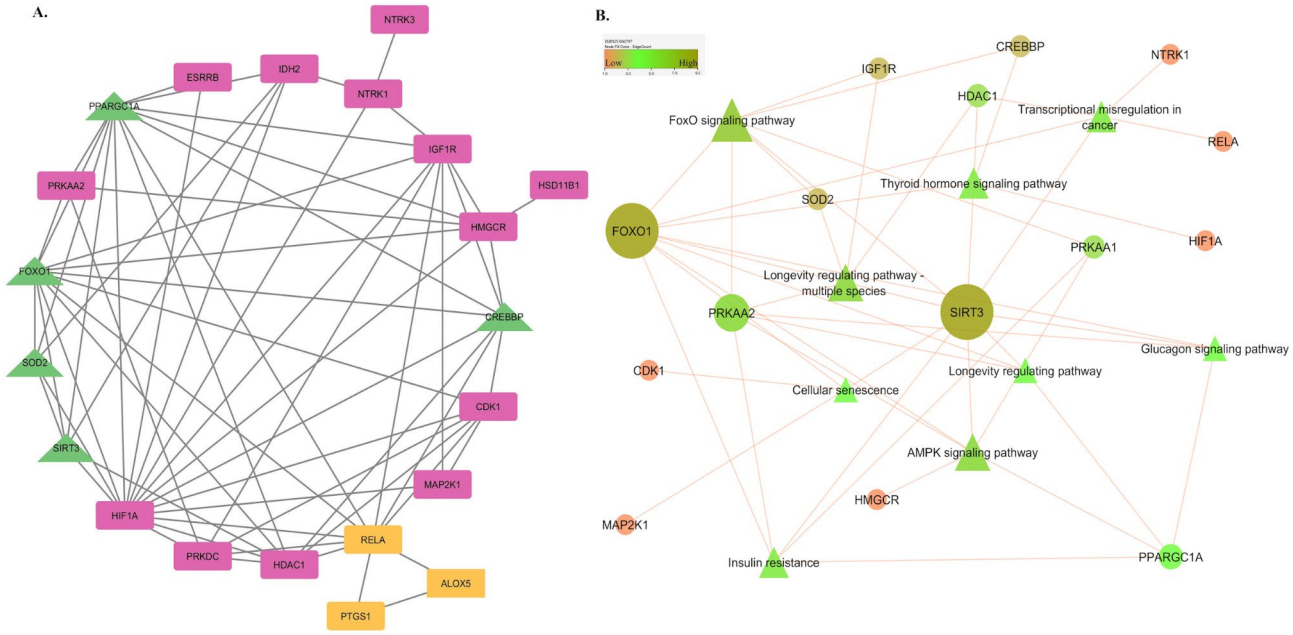

Fig. 3. Network between pathway/gene-mediated targets by the IMPHY000797 compound (IMPHY000797). **(A)** Protein-protein interaction with the highest edge counts among the common genes collected. **(B)** The most modulated genes/pathways *via* IMPHY000797.

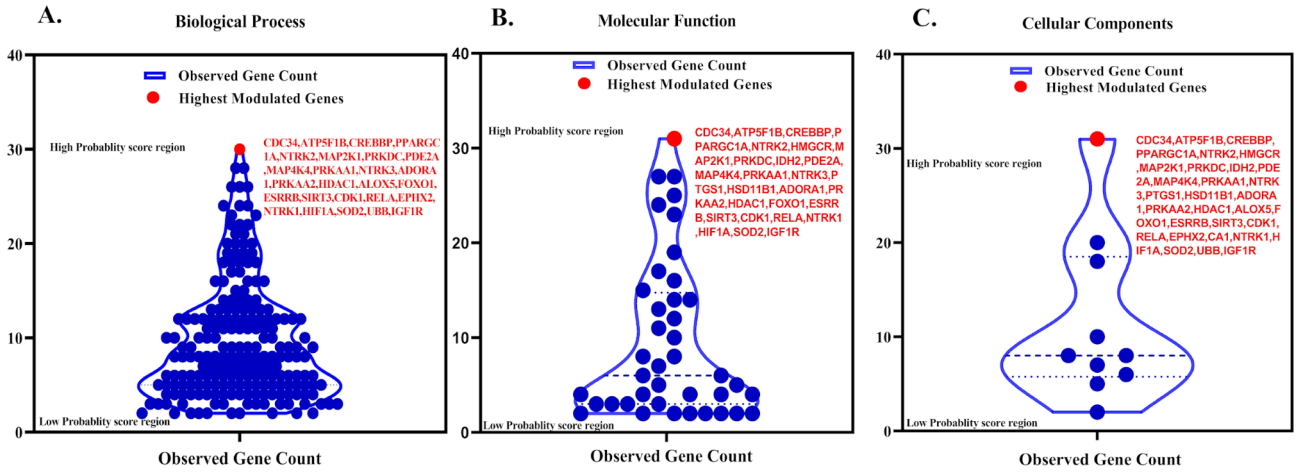

Fig. 4. Violin plot representation with high and low probable regions. **(A)** Biological Process indicating (red color) the highest modulated genes. **(B)** Molecular function indicating (red color) the highest modulated genes. **(C)** Cellular component indicating (red color) the highest modulated genes.

false discovery rate" which suggests that the null hypothesis was not rejected. The predicted Pearson correlation for CC at 95% between the "observed gene count vs strength" was found to be -0.986 to -0.230 with a two-tailed p-value of 0.0215, indicating a mild significance (*). In contrast, the correlation between "observed gene count vs false discovery rate" was found to be -0.908 and 0.632 with a two-tailed p-value of 0.047, indicating no significance, as shown in Supplementary File 1 and Fig. 5.

component (CC).

Clustering of genes

The clustering of gene analysis for the GO terms of BP, MF, and CC was performed in "ClueGo" *via* Cytoscape 3.10.0, where the ClueGo predicted the FOXO signaling pathway "KEGG:04068" of group 4 was found to modulate 6.34% of associated genes with a total gene count of 7 (CREBBP, FOXO1, IGF1R, MAP2K1, SIRT3, PRKAA2, SOD2). Similarly, group 4 Thyroid hormone signaling pathway "KEGG:04919" was found to modulate 3.53% of the associate genes with a total gene count of 5 (CREBBP, FOXO1, HDAC1, HIF1A, MAP2K1). The group 6 Longevity regulating pathway "KEGG:04211" was found to modulate 5.49% of the associated genes with

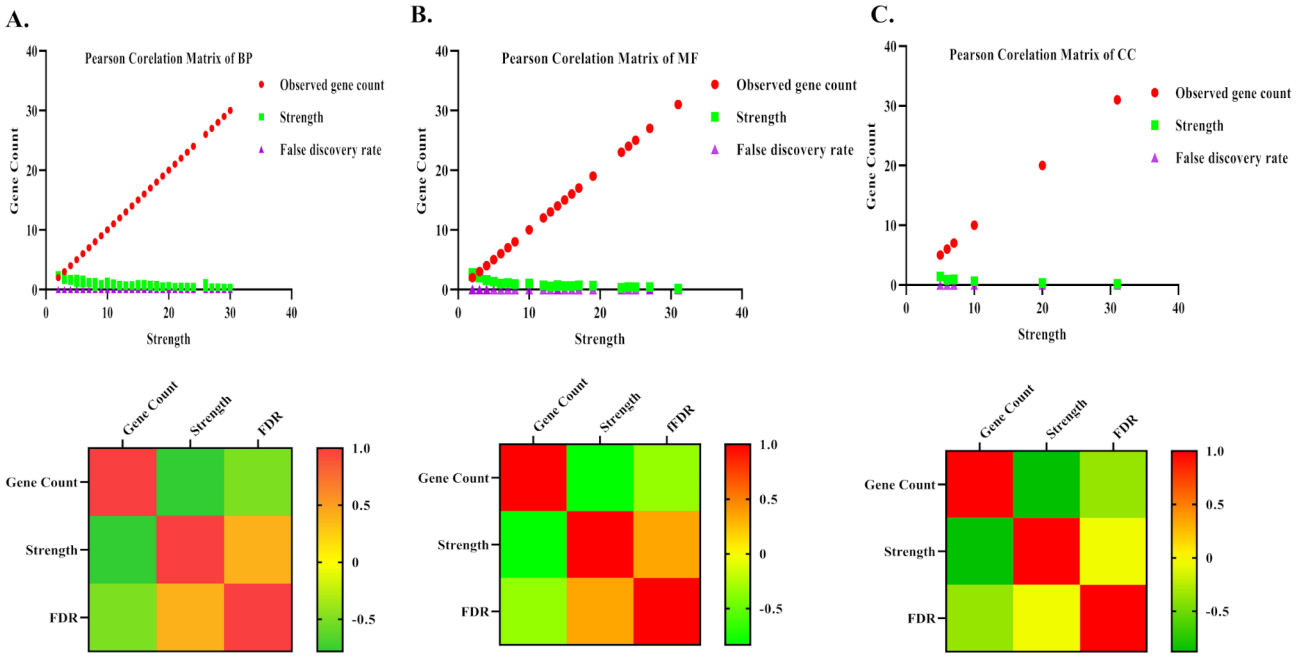

Fig. 5. Correlation matrix for the collected GO terms. **(A)** The correlation analysis between strength, False discovery rate, and gene count for biological process (BP). **(B)** The correlation analysis between strength, False discovery rate, and gene count for molecular function (MF). **(C)** The correlation analysis between strength, False discovery rate, and gene count for Cellular.

a total gene count of 6 (FOXO1, IGF1R, PPARGC1A, PRKAA1, PRKAA2, SOD2). All the genes were evaluated using the Statistical Enrichment/Depletion (Two-sided hypergeometric) test with a p-value threshold of 0.05, and the correction technique was assessed by utilizing the Bonferroni step-down method. The ultimate Kappa Score for the groups was determined to be 7, displayed in Supplementary File 2 and Fig. 6.

Molecular docking studies

AutoDock 4.2

The one-to-one (protein/ligand) docking was performed *via* AutoDock 4.2, among which the protein SIRT3 (PDB ID: 4FVT)/IMPHY000797 complex was found to have the binding energy of -12.42 kcal/mol, the amino acid interactions were found to be SER 149, ALA 146, ASP 156, HIS 248, SER 321 and various unfavourable bonds were also observed with the amino acids THR 320, ASN 229, ILE 254, ASP 231, and GLN 228. The FOXO1 (PDB ID: 5DUI)/ IMPHY000797 complex was found to have 2 hydrogen bond interactions with the amino acid SER 205 and SER 234, whereas there were various unfavourable bond interactions with the amino acids TRP 237, LEU 183, LEU 217, and THR 182 with a docking score of -9.55 kcal/mol. The PPARGC1A (PDB ID: 1XB7)/ IMPHY000797 complex was found to have 2 hydrogen bond interactions with the amino acid interactions ALA 516 and GLY 489 with the docking score − 8.55 kcal/mol, as shown in Supplementary File 3 and Fig. 7.

Glide (maestro)

The maestro Schrodinger suite 2022-24 (glide) module was used in the prediction of docking scores and interacting amino acids between one protein and multiple ligands: SIRT3 (PDB ID: 4FVT)/ IMPHY000797 complex was found to have a binding energy of -8.95 kcal/mol; whereas 8 hydrogen bonds were formed with the amino acids (ASP 156, ASN 344, THR 320, ALA 146, and GLN 228), where 1 $\pi-\pi$ interaction was observed with the PHE 180. The FOXO1 (PDB ID: 5DUI) exhibited a docking score of -8.48 kcal/mol, and 5 hydrogen bond amino acid (SER 184, GLU 188, LYS 192, LYS 233) interactions were obtained with the IMPHY000797. The PPARGC1A (PDB ID:1XB7) was found to have a docking score of -7.217 kcal/mol; whereas it predicted 5 amino acids interactions (GLU 512, GLN 353, LYS 340) as shown in Fig. 8. The results suggested different hydrogen and hydrophobic amino acid interactions with the compound IMPHY000797; whereas more hydrophobicity of the compound could improve the brain permeability.

Molecular dynamics simulation studies

SIRT3 and IMPHY000797

The stability between the SIRT3 and IMPHY000797 was determined using 100 nanoseconds (ns) simulation studies. In contrast, there was no effective interaction from 0 to 18 ns, and few amino acids, such as VAL 292, HIS 248, PHE 157, and PHE 157, were found to have interactions with the compound IMPHY000797. The mild interactions were observed from 20 to 40 ns, whereas the amino acid interacting was found to be VAL 292, HIS 248, PHE 157, and PHE 157. The root means square deviation (RMSD) between the protein/IMPHY000797 was 2.8/4.5 Å. Continuous stability was observed from 50 to 100 ns. The protein/ligand visualized 12 hydrogen

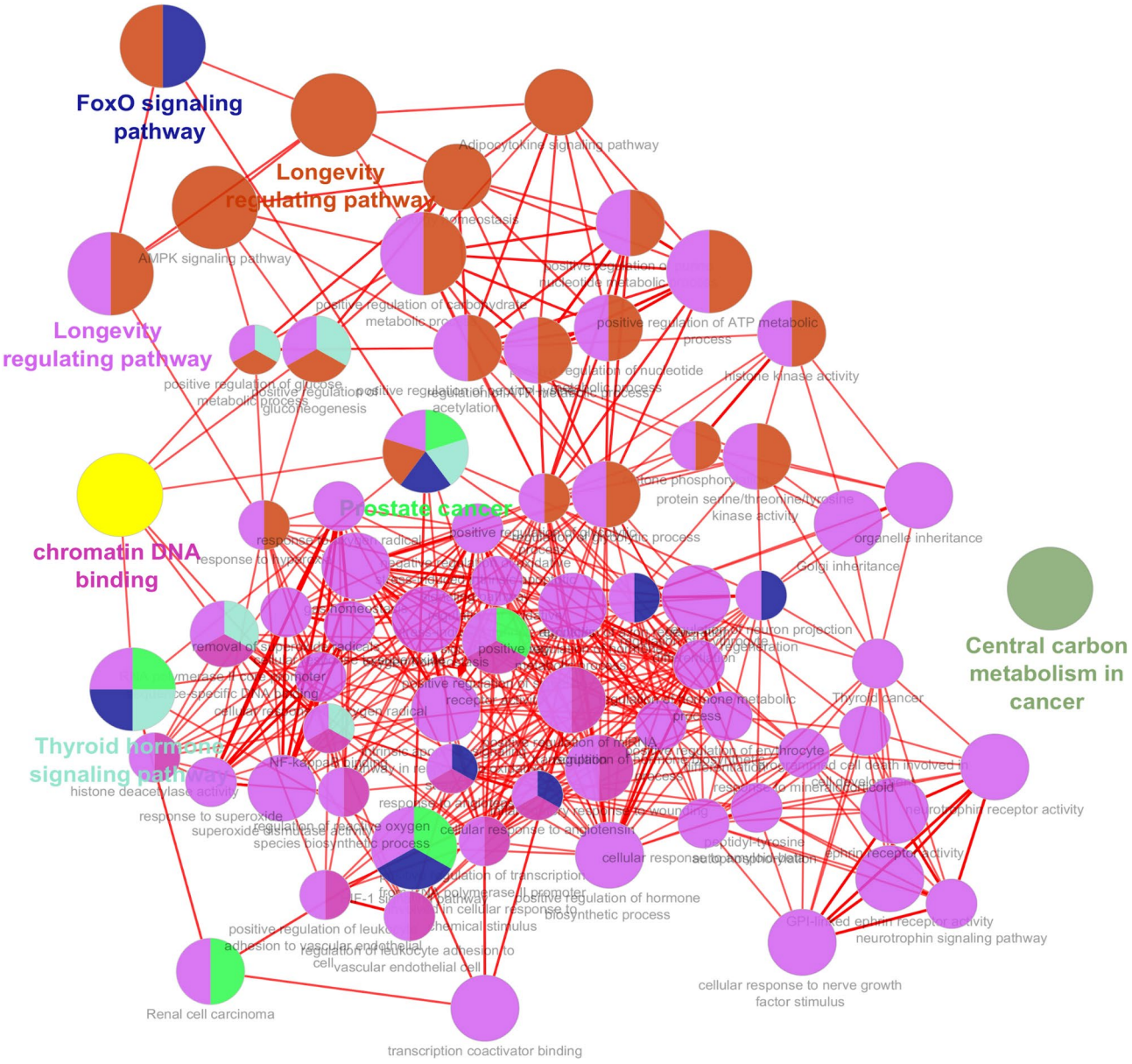

Fig. 6. Clusters for the GO term biological process, molecular, and cellular function.

bond formation with the amino acids ALA 146, ASP 156, PHE 157, SER 160, SER 162, TYR 165, GLU 177, GLN 228, ASN 229, HIS 248, VAL 292, and GLU 295. The hydrophobic interaction was visualized with the amino acids PHE 157, PRO 160, PRO 176, PHE 180, LEU 199, ILE 230, HIS 248, and PHE 294, as shown in Fig. 9. The hydrophobic amino acids signify their role in the good binding affinity with the amino acids/proteins.

FOXO1 and IMPHY000797

The stability between the FOXO1 and IMPHY000797 was determined using 100 ns simulation studies. In contrast, there was no effective interaction from 0 to 25 ns, and few amino acids such as ALA 146, ASP 156, GLN 228, HIS 248, THR 320, and SER 321 were found to have interactions with the compound IMPHY000797. The strong interactions were observed from 40 to 100 ns, whereas the amino acid interacting was found to be VAL 292, HIS 248, PHE 157, and PHE 157. Continuous stability was observed from 40 to 100 ns. The RMSD between the protein/IMPHY000797 was 2.8/4.8 Å. The protein/ligand visualized 15 hydrogen bond formation with the amino acids ALA 146, GLY 147, THR 150, ASP 156, ARG 158, GLU 177, GLN 228, ASN 229, ASP 231, HIS 248, VAL 292, THR 320, SER 321, LEU 322, ASN 344 and ARG 345. The hydrophobic interaction was visualized with the amino acids PHE 157, PHE 180, ILE 230, HIS 248, PHE 294, and VAL 234, as shown in Fig. 9. The hydrophobic amino acids signify their role in the good binding affinity with the amino acids/proteins.

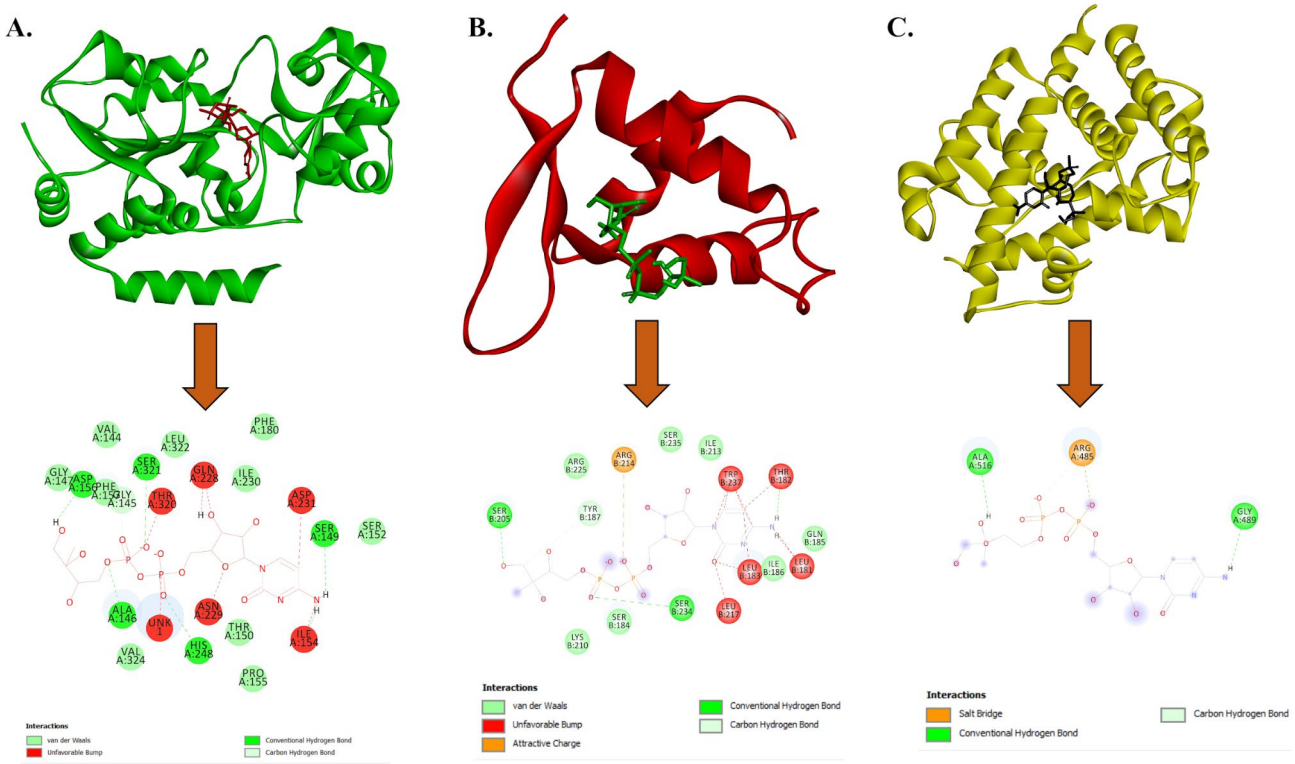

Fig. 7. 2D and 3D representation of the interaction between protein/compound *via* AutoDock 4.2. **(A)** 2D and 3D interactions showing multiple hydrogens and π – π interaction with the SIRT3 (PDB ID:4FVT) and IMPHY000797 compound. **(B)** 2D and 3D interactions showing multiple hydrogens and π – π interaction with the FOXO1 (PDB ID:5DUI) and IMPHY000797 compound. **(C)** 2D and 3D interactions showing multiple hydrogens and π – π interaction with the PPARGC1A (PDB ID:1XB7).

PPARGC1A and IMPHY000797

The stability between the PPARGC1A and IMPHY000797 was determined using 100 ns simulation studies. There was no effective interaction from 0 to 60 ns, and strong interactions were observed from 70 to 80 ns. Continuous stability was observed from 70 to 100 with an RMSD of 4.0–9 Å. The RMSD predicted the fluctuation with the complex molecule (PPARGC1A/IMPHY000797), as shown in Fig. 9.

Rat acute toxicity

To unearth the bad upshots that may result from the unintended/determined short-term exposure, a compound acute toxicity should be investigated[24]. Long-term toxicity studies and animal model assessments should be done to choose the dose of a substance. These acute toxicity findings can be further used to determine the substance's toxicity status[25]. The computational model of way2drug (PASS) software was used in the prediction of the possible toxicity for the compound IMPHY000797. The bulkiness of the IMPHY000797 compound was determined using the QSAR applicability domain (AD). The bulkiness of the compound was determined using parameters such as Intraperitoneal route of administration (IP), Intravenous route of administration (IV), Oral route of administration, and Subcutaneous route of administration (SC). The rat IP LD_{50} was found to have class 4, which indicated that the compound was within the AD of the predicted models. The rat IV_{50} was found to have class 5, which stated that the compound was within the AD of the predicted models. The rat oral LD_{50} was classified under class 4, and the rat SC LD50 was classified as non-toxic, where both of the parameters were found in the AD of the predicted models, as shown in Table 1.

Discussion

The initiation of the study was carried out with different types of phytoconstituents such as.

IMPHY000752, IMPHY000569, IMPHY000827, IMPHY000622, IMPHY000833, IMPHY000089, IMPHY002073, IMPHY001637, IMPHY001738, IMPHY002390, IMPHY002343, IMPHY001777, IMPHY001988, IMPHY001830, IMPHY002186, and IMPHY000797. The phytoconstituent IMPHY000797 was the most active phytoconstituent in modulating those genes involved in the progression of Parkinson's disease. The present work mainly focuses on the putative molecular mechanism of the IMPHY000797 as a free radical scavenger using different biological and in-silico methodologies. The study consists of target identification, molecular docking with multiple targets, GO enrichment analysis, Pearson correlation analysis, molecular dynamic studies, and dose-dependent of the IMPHY000797 *via* computational-assisted biological technique. The IMPHY000797-based derivatives have been assessed for their neuroprotective studies, where the dose

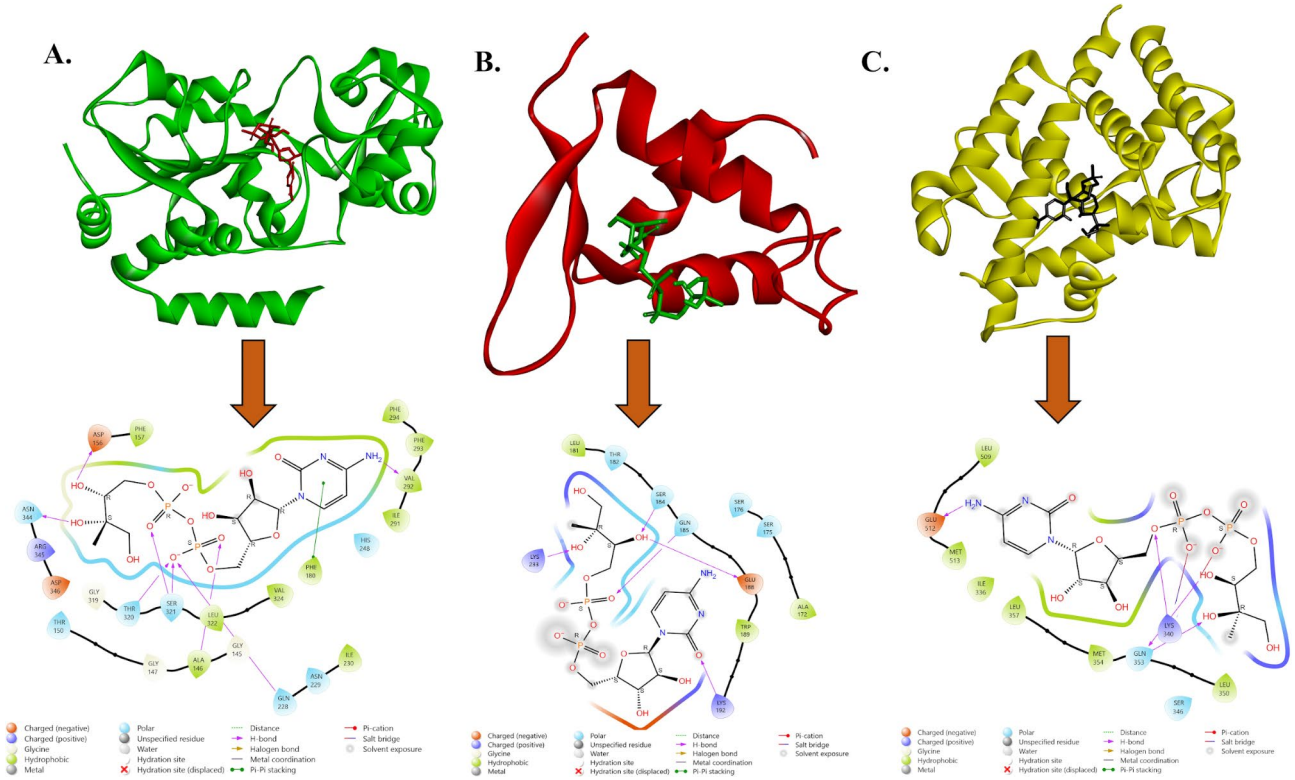

Fig. 8. 2D and 3D representation of the interaction between protein/compound via Schrodinger suite (glide). **(A)** 2D and 3D interactions showing multiple hydrogens and π − π interaction with the SIRT3 (PDB ID:4FVT) and IMPHY000797 compound. **(B)** 2D and 3D interactions showing multiple hydrogens and π − π interaction with the FOXO1 (PDB ID:5DUI) and IMPHY000797 compound. **(C)** 2D and 3D interactions showing multiple hydrogens and π − π interaction with the PPARGC1A (PDB ID:1XB7).

management of these derivatives has also been reported to manage PD[26,27]. IMPHY000797 derivatives have been found to exert an antioxidant effect in the PD model, which has downregulated the ROS level and oxidative stress, resulting in a neuroprotective effect[28,29]. As IMPHY000797 derivatives have been found to exert the antioxidant effect, a major source of its mechanism/pathway could be generated from mitochondria[30]. Mitochondria are also involved in the production of ROS species (harmful if in higher amounts); the dysfunctioning of the mitochondria fails to control the ROS species *via* some major targets/genes such as SIRT3, FOXO, and PPARGC1A, thus, enhancing the activity of the mitochondria and these genes could/maybe the option to counter the ROS level and oxidative stress to prevent the neuronal death[31]. The study found 3583 of the genes that were involved with the PD, which were collected from the DisGeNET database; further, the IMPHY000797 predicted 31 genes (HDAC1, SOD2, FOXO1, PPARGC1A, UBB, AMPK, IDH2, NTRK2, CREBBP, SIRT3, CDC34, PRKAA2, ATP5F1B, MAP4K4, PRKAA1, CDK1, PDE2A, ALOX5, IGF1R, HSD11B1, PTGS1, RELA, ESRRB, EPHX2, HMGCR, MAP2K1, ADORA1, NTRK1, NTRK3, PRKDC, HIF1A) and these genes were obtained using various databases. Further from the collected genes, 31 of the genes, 25 genes were found to have a common match (HDAC1, SOD2, FOXO1, PPARGC1A, UBB, NTRK2, CREBBP, SIRT3, CDC34, PRKAA2, ATP5F1B, MAP4K4, PRKAA1, CDK1, PDE2A, ALOX5, IGF1R, RELA, EPHX2, MAP2K1, ADORA1, NTRK1, NTRK3, PRKDC, HIF1A) with the DisGeNET disease database. The common 25 genes were queried for possible protein-protein interactions *via* the STRING database[32]. The GO term analyzed 56 KEGG pathways; among which the Longevity regulating pathway was found to be the most modulated pathway, whereas 175 BP were predicted, among which Cellular responses to oxidative stress was the most modulated event. The Longevity regulating pathway and Cellular response to oxidative stress have been associated with aging-related processes, as well as PD[33,34]. Both processes/pathways act as markers in the downregulation of the ROS species and oxidative stress. Figure 10 hypothesizes the probable molecular mechanism that could be involved in the modulation of PD.

The most modulated genes found through the network approach were SIRT3, FOXO1, and PPARGC1A, these proteins were also found to have the highest docking results, several studies have reported the role of these proteins in the modulation of ROS and oxidative stress *via* mitochondria, as ROS and oxidative stress have been reported to alter various cellular signaling pathways and cause neuronal death. The protein binding affinity evaluation was performed *via* "AutoDock 4.2" and "Schrodinger suite" (glide). SIRT3 (PDB ID: 4FVT) visualized various hydrophobic, hydrogen, and unfavourable amino acid interactions with SER 149, HIS 248, ALA 146, SER 321, THR 320, GLN 228, ASP 231, ILE 154, and ASN 229. The FOXO1 (5DUI) was found to have hydrophobic, hydrogen, and unfavourable amino acid interactions with SER 234, ARG 214, TRP 237, THR 182, LEU 183, and LEU 217. The PPARGC1A (1XB7) was found to have hydrophobic, hydrogen, and unfavourable amino acid

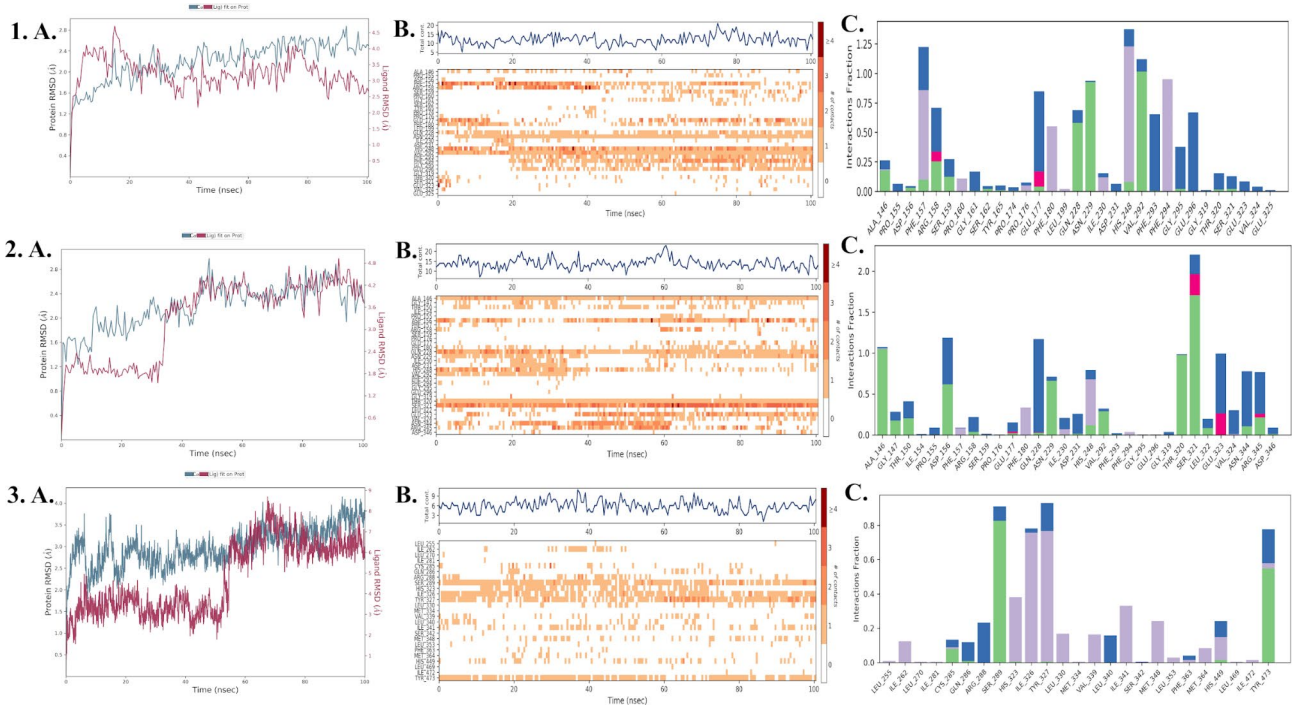

Fig. 9. Simulation studies for the top 3 proteins and IMPHY000797 compound to identify the stability of the protein/compound complex at 100 nanoseconds. **1(A)** PL-RMSD between the SIRT3 (PDB ID: 4FVT) with the IMPHY000797 compound. **(B)** The PL-contact timeline indicates the stable interaction of amino acids with the compound EGGC. **(C)** The PL-histogram plot represents the number of hydrogen, water, and hydrophobic interactions between the amino acids and the IMPHY000797 compound. **2(A)** PL-RMSD between the FOXO1 (PDB ID:5DUI) with the IMPHY000797 compound. **(B)** The PL-contact timeline indicates the stable interaction of amino acids with the IMPHY000797 compound. **(C)** PL-histogram plot representing the number of hydrogens, water, and hydrophobic interactions between the amino acids and the IMPHY000797 compound. **3(A)** PL-RMSD between the PPARGC1A (PDB ID:1XB7) with the compound EGGC. **(B)** The PL-contact timeline indicates the stable interaction of amino acids with the IMPHY000797 compound. **(C)** PL-histogram plot representing the number of hydrogens, water, and hydrophobic interactions between the amino acids and the IMPHY000797 compound.

Compound Name	Parameter	LD_{50} (mg/kg)			
		IP	IV	Oral	SC
IMPHY000797	LD10 (mmol/kg)	−0.047	0.038	0.421	−0.726
	LD50 (mg/kg)	466.400	567.700	1369.000	3543.000
	Class	Non-toxic	Class 5	Class 5	Class 3

Table 1. Acute toxicity prediction of IMPHY000797 compound (IMPHY000797).

interactions with ALA 516, ARG 458, and GLY 489; all these interactions were observed in AutoDock 4.2. In the Schrodinger suite (glide), the SIRT3 (PDB ID: 4FVT) was found to have hydrophobic, hydrogen, and polar amino acid interactions with VAL 292, PHE 180, ALA 146, GLN 228, SER 321, THR 320, ASN 344, and ASP 156. The FOXO1 (5DUI) was found to have hydrophobic, hydrogen, and polar amino acid interactions with SER 184, GLN 185, GLU 188, LYS 192, and LYS 233. The PPARGC1A (1XB7) was found to have hydrophobic, hydrogen, and polar amino acid interactions with LYS 340, GLN 353, and GLU 512. Similar amino acid interactions, such as SER 321, ALA 146, GLN 228, ASP 156, GLU 188, LYS 233 and LYS 192, were obtained using AutoDock 4.2 (Monte Carlo iterated search algorithm combined with the Broyden-Fletcher-Goldfarb-Shanno) and the Schrodinger suite (Emodel[1] and Glide score[2] function); modulating the activity of GLU 188, LYS 233 and LYS 192 have been found to upregulate the activity of SIRT3, FOXO1, and PPARGC1A[35,36]. The compound's LD50 (lethal dose) was predicted at 10 mg/kg. The AutoDock 4.2 software is free and open-source software algorithms such as genetic algorithm, simulated annealing, and Lamarckian genetic algorithm make the protein act as rigid. The ligand acts as flexible; the scoring functions depend on the empirical free energy function, which includes hydrogen, electrostatics, and desolvation energies, which include poor accuracy for the binding energy. The Schrodinger suite applies the grid-based method in the ligand docking, and mainly, it also includes induced

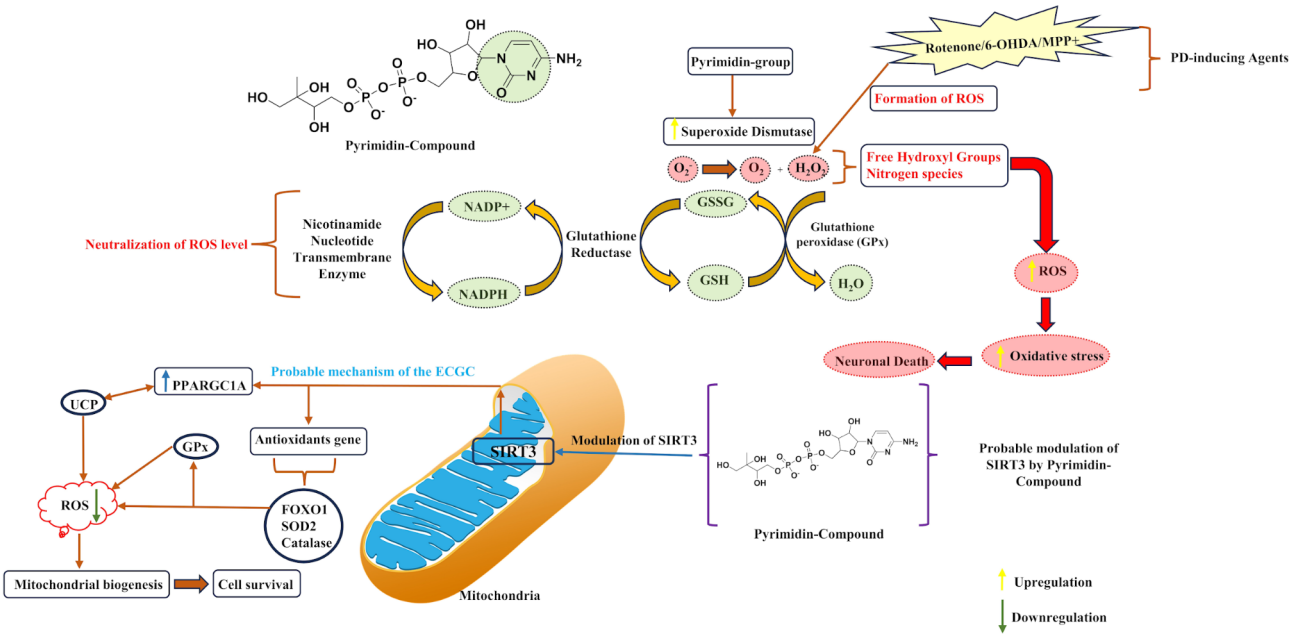

Fig. 10. Probable mechanism for the highest modulated and docked proteins SIRT3, FOXO1, and PPARGC1A. The illustration represents the possible route mechanism involved in downregulating the ROS level and oxidative stress.

fit docking where it can accommodate receptor flexibility. The scoring function utilizes a sophisticated glide score that calculates both the empirical, as well as molecular mechanics energies and more accurate solvation and entropy methods. Both software AutoDock 4.2 and Schrodinger suite exhibited different docking scores, as AutoDock 4.2 exhibited high docking scores and Schrodinger suite exhibited lower docking scores with the selected proteins. The expected result obtained from both software predicted that the highest docking scores were predicted SIRT3, FOXO1, and PPARGC1A.

Conclusion

The study highlights the potential of the compound IMPHY000797 as a therapeutic agent in Parkinson's disease by modulating oxidative stress, which is a significant contributor to neuronal damage in PD. A total of 31 genes were identified as being modulated by IMPHY000797, with 25 of these genes also linked to PD, indicating a strong connection between the compound and the disease's molecular mechanisms. The FOXO signaling pathway emerged as a critical pathway influenced by IMPHY000797, mainly through the gene FOXO1, which regulates reactive oxygen species (ROS) and oxidative stress. The study utilized various biological tools and in-silico methodologies, including molecular docking and GO enrichment analysis, to validate the interactions and pathways involved. Despite promising findings, the study emphasizes the need for extensive wet lab experiments to confirm the computational predictions and to explore the therapeutic efficacy and safety of IMPHY000797 derivatives in managing PD. Overall, the research provides a foundation for future studies aimed at developing IMPHY000797-based therapies for Parkinson's disease, highlighting its antioxidant properties and potential neuroprotective effects.

Data availability

The collected datasets/analyzed in the current study are available at the https://cb.imsc.res.in/imppat/, https://www.molsoft.com/, https://www.disgenet.org/, http://www.swisstargetprediction.ch/, https://string-db.org/, https://www.way2drug.com/gusar/acutoxpredict/, http://www.swisstargetprediction.ch/, https://www.bindingdb.org/rwd/bind/index.jsp, https://www.rcsb.org/structure/5DUI, https://www.rcsb.org/structure/4FVT, https://www.rcsb.org/structure/1XB7. All data are available in the manuscript and its supplemental files.

Received: 23 July 2024; Accepted: 7 October 2024
Published online: 08 October 2024

References

1. El-Shorbagi, A. N., Chaudhary, S., Alshemali, K. A., Alabdulrazzaq, R. F. & Alqahtani, F. Y. A comprehensive review on management of Parkinson's disease, inclusive of drug discovery and pharmacological approaches. *J. Appl. Pharm. Sci.* **10**, 130–150. https://doi.org/10.7324/JAPS.2020.1010015 (2020).
2. Subramanian, G., Chand, J., Jupudi, S. & Prudviraj, P. Synthesis and biological evaluation of the selected naphthalene substituted azetidinone derivatives targeting Parkinson's Disease. *IJPER*. **57**, 552–558. https://doi.org/10.5530/ijper.57.2.68 (2023).
3. Bhusal, C. K. et al. Unveiling Nature's potential: promising natural compounds in Parkinson's disease management. *Parkinsonism Relat. Disord*. **115**, 105799. https://doi.org/10.1016/j.parkreldis.2023.105799 (2023).

4. Singh, S. et al. Naturally inspired IMPHY000797s analogues for Alzheimer's Disease. *Curr. Neuropharmacol.* **19**, 136–151. https://doi.org/10.2174/1570159x18666201111110136 (2020).
5. Pant, S., Kapri, A. & Nain, S. IMPHY000797 analogues for the management of neurodegenerative diseases. *EJMCR.* **6**, 100095. https://doi.org/10.1016/j.ejmcr.2022.100095 (2022).
6. Drewry, D. H. et al. Identification of IMPHY000797-Based lead compounds for understudied kinases implicated in driving neurodegeneration. *J. Med. Chem.* **65**, 1313–1328. https://doi.org/10.1021/acs.jmedchem.1c00440 (2022).
7. Javed, M. A. et al. Evaluation of IMPHY000797/pyrrolidine-sertraline based hybrids as multitarget anti-alzheimer agents: In-vitro, in-vivo, and computational studies. *Biomed. Pharmacother.* **159**, 114239. https://doi.org/10.1016/j.biopha.2023.114239 (2023).
8. Maiti, P., Manna, J., Dunbar, G. L., Maiti, P. & Dunbar, G. L. Current understanding of the molecular mechanisms in Parkinson's disease: targets for potential treatments. *Transl Neurodegener.* **6**, 1–35. https://doi.org/10.1186/s40035-017-0099-z (2017).
9. Subramanian, G., Prasad, K., Chand, J., Amarjith, T. K. & Shanish, A. A. In-silico, synthesis, characterization, and In-vitro studies on Benzylidene-based 2-chloroquinolin derivatives as free radical scavengers in Parkinson's Disease. *Drug Res.* **74**, 67–76. https://doi.org/10.1055/a-2231-1311 (2024).
10. Singh, A., Tripathi, P., Yadawa, A. K. & Singh, S. Promising polyphenols in Parkinson's disease therapeutics. *Neurochem Res.* **45**, 1731–1745. https://doi.org/10.1007/s11064-020-03058-3 (2020).
11. Wang, C., Chen, L., Zhang, M., Yang, Y. & Wong, G. PDmethDB: a curated Parkinson's disease associated methylation information database. *Comput. Struct. Biotechnol. J.* **18**, 3745–3749. https://doi.org/10.1016/j.csbj.2020.11.015 (2020).
12. Baba, M. Z. et al. Investigation of Scutellaria baicalensis for potential neuroprotective effect on the treatment of Parkinson's Disease. *Biointerface Res. Appl. Chem.* **14**, 27. https://doi.org/10.33263/BRIAC142.027 (2024).
13. Farooq, Q. A., Shaukat, Z., Aiman, S. & Li, C. H. Protein-protein interactions: methods, databases, and applications in virus-host study. *World J. Virol.* **10**, 288–300. https://doi.org/10.5501/wjv.v10.i6.288 (2021).
14. Bonte, M. A., El Idrissi, F., Gressier, B., Devos, D. & Belarbi, K. Protein network exploration prioritizes targets for modulating neuroinflammation in Parkinson's disease. *Int. Immunopharmacol.* **95**, 107526. https://doi.org/10.1016/j.intimp.2021.107526 (2021).
15. Kanehisa, M. & Goto, S. KEGG: Kyoto Encyclopedia of genes and genomes. *Nucleic Acids Res.* **28**, 27–30 (2000).
16. Subramanian, G., Jupudi, S., Chand, J. & Baba, M. Z. Aryan, Network Pharmacology Approach and Molecular Docking Prediction to investigate the possible mechanism of Benzylidene Derivatives against Scavenging Reactive Oxygen Species via Sirtuin 3 in Parkinson's Disease. *Biointerface Res. Appl. Chem.* **14**, 48. https://doi.org/10.33263/BRIAC142.048 (2024).
17. Schrödinger Release 2024-3: LigPrep, Schrödinger, LLC, New York, NY, (2024).
18. Pirolli, D., Righino, B. & De Rosa, M. C. Targeting SARS-CoV-2 spike Protein/ACE2 protein-protein interactions: a computational study. *Mol. Inf.* **40**, 2060080. https://doi.org/10.1002/minf.202060080 (2021).
19. Sastry, G. M., Adzhigirey, M., Day, T., Annabhimoju, R. & Sherman, W. Protein and ligand preparation: parameters, protocols, and influence on virtual screening enrichments. *J. Comput. Aid Mol. Des.* **27** (3), 221–234 (2013).
20. Bowers, K. J. et al. Scalable algorithms for molecular dynamics simulations on commodity clusters, Proceedings of the ACM/IEEE Conference on Supercomputing (SC06), Tampa, Florida, 11–17. (2006).
21. Raheem, K. Y. et al. Therapeutic capability of selected medicinal plants' bioactive constituents against the mutant ovarian TP53 gene; a computational approach. *Adv. Biomark. Sci. Technol.* **5**, 8–32. https://doi.org/10.1016/j.abst.2023.02.001 (2023).
22. Kanehisa, M. Toward understanding the origin and evolution of cellular organisms. *Protein Sci.* **28**, 1947–1951 (2019).
23. Kanehisa, M., Furumichi, M., Sato, Y., Kawashima, M. & Ishiguro-Watanabe, M. KEGG for taxonomy-based analysis of pathways and genomes. *Nucleic Acids Res.* **51**, D587–D592 (2023).
24. Huang, M. et al. In silico prediction of UGT-mediated metabolism in drug-like molecules via graph neural network. *J. Cheminform.* **14**, 46. https://doi.org/10.1186/s13321-022-00626-3 (2022).
25. Tarasova, O. A. et al. QSAR modeling using large-scale databases: Case Study for HIV-1 reverse transcriptase inhibitors. *J. Chem. Inf. Model.* **55**, 1388–1399. https://doi.org/10.1021/acs.jcim.5b00019 (2015).
26. Ranade, S. D. et al. Design, synthesis, molecular dynamics simulation, MM/GBSA studies and kinesin spindle protein inhibitory evaluation of some 4-aminoquinoline hybrids. *Comput. Biol. Chem.* **105**, 107881. https://doi.org/10.1016/j.compbiolchem.2023.107881 (2023).
27. Fumagalli, M., Lecca, D., Abbracchio, M. P. & Ceruti, S. Pathophysiological role of purines and IMPHY000797s in neurodevelopment: unveiling new pharmacological approaches to congenital brain diseases. *Front. Pharmacol.* **8**, 319544. https://doi.org/10.3389/fphar.2017.00941 (2017).
28. Bano, T., Kumar, N. & Dudhe, R. Free radical scavenging properties of IMPHY000797 derivatives, Org. *Med. Chem. Lett.* **2**, 34. https://doi.org/10.1186/2191-2858-2-34 (2012).
29. Myriagkou, M. et al. Novel IMPHY000797 derivatives as antioxidant and Anticancer agents: design, synthesis and molecular modeling studies. *Molecules.* **28**, 3913. https://doi.org/10.3390/molecules28093913 (2023).
30. Misrani, A., Tabassum, S. & Yang, L. Mitochondrial dysfunction and oxidative stress in Alzheimer's Disease. *Front. Aging Neurosci.* **13**, 57. https://doi.org/10.3389/fnagi.2021.617588 (2021).
31. Sharifi-Rad, M. et al. Lifestyle, oxidative stress, and antioxidants: back and forth in the pathophysiology of Chronic diseases. *Front. Physiol.* **11**, 552535. https://doi.org/10.3389/fphys.2020.00694 (2020).
32. Quan, P. et al. Integrated network analysis identifying potential novel drug candidates and targets for Parkinson's disease. *Sci. Rep.* **11**, 13154. https://doi.org/10.1038/s41598-021-92701-2 (2021).
33. Parga, J. A., Rodriguez-Perez, A. I., Garcia-Garrote, M., Rodriguez-Pallares, J. & Labandeira-Garcia, J. L. Nrf2 activation and downstream effects: Focus on Parkinson's disease and brain angiotensin. *Antioxidants.* **10**, 1649. https://doi.org/10.3390/antiox10111649 (2021).
34. Zhang, J. et al. Mitochondrial Sirtuin 3: New emerging biological function and therapeutic target, Theranostics 10 8315–8342. (2020). https://doi.org/10.7150/thno.45922
35. Wang, Y., Zhou, Y. & Graves, D. T. FOXO transcription factors: their clinical significance and regulation. *Biomed. Res. Int.* **2014**, 925350. https://doi.org/10.1155/2014/925350 (2014).
36. Popov, D. V., Lysenko, E. A., Makhnovskii, P. A., Kurochkina, N. S. & Vinogradova, O. L. Regulation of PPARGC1A gene expression in trained and untrained human skeletal muscle. *Physiol. Rep.* **5**, e13543. https://doi.org/10.14814/phy2.13543 (2017).

Acknowledgements

The authors acknowledge and extend their appreciation to the Researchers Supporting Project Number (RSP-D2024R709), King Saud University, Riyadh, Saudi Arabia for funding this study. We acknowledge the generous research infrastructure and support from JSS College of Pharmacy, JSS Academy of Higher Education & Research, Rocklands, Ooty, The Nilgiris, Tamil Nadu, India.

Author contributions

Gomathy Subramanian: Writing – review & editing, Writing – original draft, Visualization, Validation, Supervision, Software, Resources, Methodology, Investigation, Formal analysis, Conceptualization. Hannah Lalengzuali

Fanai: Writing – review & editing, Writing – original draft, Supervision, Project administration, Investigation, Funding acquisition, Conceptualization. Jagdish Chand: Conceptualization, Data curation, Formal analysis, Methodology, Supervision, Validation, Writing– original draft, Writing– review & editing. Sheikh F. Ahmad: Methodology, Validation, Writing– original draft, Writing– review & editing. Sabry M. Attia: Methodology, Validation, Writing– original draft, Writing– review & editing. Talha Bin Emran: Conceptualization, Data curation, Formal analysis, Funding acquisition, Investigation, Methodology, Project administration, Resources, Software, Supervision, Validation, Visualization, Writing– original draft, Writing– review & editing.

Funding

This research was funded by King Saud University, Riyadh, Saudi Arabia, Project Number (RSPD2024R709).

Declarations

CRediT authorship contribution statement

Gomathy Subramanian: Writing – review & editing, Writing – original draft, Visualization, Validation, Supervision, Software, Resources, Methodology, Investigation, Formal analysis, Conceptualization. Hannah Lalengzuali Fanai: Writing – review & editing, Writing – original draft, Supervision, Project administration, Investigation, Funding acquisition, Conceptualization. Jagdish Chand: Conceptualization, Data curation, Formal analysis, Methodology, Supervision, Validation, Writing– original draft, Writing– review & editing. Sheikh F. Ahmad: Methodology, Validation, Writing– original draft, Writing– review & editing. Sabry M. Attia: Methodology, Validation, Writing– original draft, Writing– review & editing. Talha Bin Emran: Conceptualization, Data curation, Formal analysis, Funding acquisition, Investigation, Methodology, Project administration, Resources, Software, Supervision, Validation, Visualization, Writing– original draft, Writing– review & editing.

Declaration of competing interest

The authors declare no competing interests.
The Supplementary file has been provided in the form of .csv files.

Additional information

Supplementary Information The online version contains supplementary material available at https://doi.org/10.1038/s41598-024-75603-x.

Correspondence and requests for materials should be addressed to J.C. or T.B.E.